

K. Baazouzi, A.D. Bensalah, S. Drid, L. Chrifi-Alaoui

Passivity voltage based control of the boost power converter used in photovoltaic system

Introduction. This paper presents a robust nonlinear control of the DC-DC boost converter feeding by a photovoltaic system based on the passivity control. The control law design uses the passivity approach. **Novelty.** The novelty consists in designing a control law for a photovoltaic system using a passivity approach based on energy shaping and associated with damping injection. **Purpose.** The purpose consists to develop a tool for design and optimize a control law of the photovoltaic system in order to improve its efficiency under some conditions such as the variations of the temperature, the irradiation and the parameters. Also, the control law design should be simple with a lower overshoot and a shorter settling time. **Methods.** This work uses the port Hamiltonian mathematical approach with minimization of the energy dissipation in boost converter of the photovoltaic system to illustrate the modification of energy and generate a specify duty cycle applied to the converter. **Results.** The results with MATLAB/SimPowerToolbox® have proven the robustness against parameter variations and effectiveness of the proposed control. **Practical value.** The experimental results, carried out using a dSPACE DS1104 system, are presented to show the feasibility and the robustness of the proposed control strategy against parameter variations. References 26, tables 3, figures 18.

Key words: DC-DC converters, interconnection and damping assignment, passivity based control, port controlled Hamiltonian.

Вступ. У статті представлено надійне нелінійне керування живленням перетворювача постійного струму, що підвищує, фотоелектричною системою на основі керування пасивністю. У створенні закону управління використовується пасивний підхід. **Новизна.** Новизна полягає у розробці закону управління фотоелектричною системою з використанням пасивного підходу, заснованого на формуванні енергії та пов'язаного з упорскуванням демпфування. **Мета.** Мета полягає в тому, щоб розробити інструмент для проектування та оптимізації закону керування фотогальванічною системою для підвищення її ефективності за деяких умов, таких як зміни температури, опромінення та параметрів. Крім того, будова закону управління має бути простою, з меншим перерегулюванням і коротшим часом встановлення. **Методи.** У роботі використовується математичний підхід Гамільтона до порту з мінімізацією розсіювання енергії у перетворювачі фотоелектричної системи, що підвищує, щоб проілюструвати зміну енергії і створити заданий робочий цикл, що застосовується до перетворювача. **Результати.** Результати з використанням MATLAB/SimPowerToolbox® довели стійкість до змін параметрів та ефективність запропонованого керування. **Практична цінність.** Представлені експериментальні результати, отримані з використанням системи dSPACE DS1104, щоб показати здійсненність та стійкість запропонованої стратегії управління при зміні параметрів. Бібл. 26, табл. 3, рис. 18.

Ключові слова: DC-DC перетворювачі, призначення взаємоз'єднань та демпфування, управління на основі пасивності, гамільтоніан, керований порт.

Introduction. Control theory has overcome the problems of dynamic systems such as uncertain, disturbed and time invariant linear models. Therefore, designing feedback controllers has become a relatively easy and efficient task [1].

However, the above described control theory is no longer applicable in case of nonlinear models. In the few past decades, several nonlinear control and stability methodologies are broadly known in the literature.

The dependence of the linear control on the operating point is raised [2, 3], on the other hand, the sliding mode control drawback is the high and free switching frequency, which generates unconfined voltages or currents [4]. The choice of the candidate function for the stabilizing control based on the Lyapunov criterion of is not obvious for the nonlinear systems it is generally heuristic [5].

The passivity control has been introduced by Romeo Ortega in 1998. It is a controller design procedure rendering the system passive and respecting the desired storage function. This guarantees the stability of the overall system [6-8].

Globally, the Passivity Based Control (PBC) can be classified on two groups, classical passivity control where the storage function is defined (typically quadratic), then design the controller that renders the storage function non-increasing. This approach is similar to a Lyapunov method. In the second passivity control group, the storage function is not defined, but instead selecting the closed-loop desired structure, and then characterizes energy functions compatible with the desired structure. The outstanding

examples of this approach are the interconnection and damping assignment (IDA) method [9].

Generally, the passivity control law can be designed according two approaches; the Lagrangian model [8-10] or the Hamiltonian approach [11, 12]. The Lagrangian form is used for mechanical as well as in electrical systems [8]. However, due to the physical characteristics of transistors and diodes used in the DC-DC converters, the Lagrangian formulation is not suitable [2, 13-15].

The goal of the paper is analysis Hamiltonian structure using interconnection and damping assignment method associated to passivity control (IDA-PBC) applied in photovoltaic system. It is a well-established technique to simplify the control law and achieve a desired equilibrium point with minimum storage energy of output voltage.

Subject of investigations. In this work the output voltage from the photovoltaic (PV) system, operate to achieve a desired output voltage of the boost converter by modifying passivity forms of port Hamiltonian model using passivity approach [11, 12]. The design and implementation control law of the output voltage is presented. With the increase of the energy demand the world turned to solar energy which is easy availability, free, inexhaustible source and without CO₂ gas emissions.

In PV panels solar cells are the basic components and it is made of silicon. A solar cell is generally a p-n junction which is made of silicon. It is made up of two different layers when a smaller quantity of impurity atoms added to it. The PV cell is a basic device of the PV system which

converts the irradiations solar to the electrical energy and provide energy to the consumer or feed power to the grid.

Many stages are used in grid connected PV system like PV array, DC to DC converter, DC to AC converter.

The converters used in the PV system are a nonlinear; they have a bilinear model such as the DC-DC boost converter.

In this paper a model is developed through converting common circuit equation of solar cell in to simplified form including the effects of changing solar irradiation and changing temperature by maximum power point tracking (MPPT) algorithm.

The originality of this work consists of the design a control law for a PV system by interconnection and damping assignment.

Modeling, relationships and assumptions. Figure 1 shows the structure of the studied system. The converter is placed between the PV array and load. It can be controlled using microcontroller or digital signal processor (DSP) in order to regulate the output voltage [16, 17].

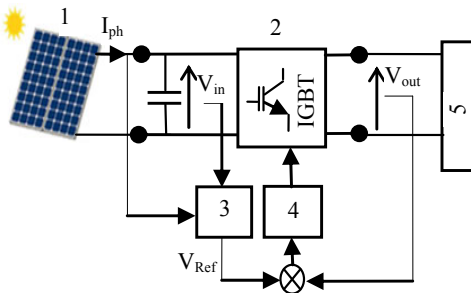


Fig. 1. PV system device with DC-DC boost drive: 1 – PV cell; 2 – DC-DC boost; 3 – MPPT; 4 – IDA-PBC controller; 5 – load

Two approaches have been developed to model the behavior of PV array. The first is based on the equivalent circuit and the second is empirically based models [15].

In the calculation, the following assumptions were made: the one diode equivalent circuit (Fig. 2) is chosen due its simplicity [18].

The main calculation relation is the equation of the PV current I_{pv} :

$$I_{pv} = I_{ph} - \frac{V_{pv} + R_s I_{pv}}{R_{sh}} - I_d \left(e^{\frac{V_{pv} + R_s I_{pv}}{aV_T}} - 1 \right), \quad (1)$$

where I_d is the current in equivalent diode; a is the diode constant; $V_T = kT/q$ is the thermal voltage; T is the temperature; k is the Boltzmann constant; q is the charge of electron; I_{ph} indicates the light current which is proportional to the irradiation G but it is affected by the temperature.

$$I_{ph} = \frac{G}{G_n} \cdot (K_I \Delta T + I_{pv,n}), \quad (2)$$

where $I_{pv,n}$ is the nominal light generated current at (25 °C – 1000 W·m⁻²), $\Delta T = T - T_n$ is the variation temperature and G_n is the nominal irradiation [W·m⁻²].

In order to take into account of the saturation current I_s is given by:

$$I_s = \frac{I_{sc,n} + K_I \Delta T}{\left(e^{\frac{V_{oc,n} + K_V \Delta T}{aV_T}} - 1 \right)}, \quad (3)$$

where I_{sc} is the short-circuit current; V_{oc} is the open circuit voltage; K_V and K_I are voltage and current coefficients.

The rate parameters of the PV panel are reported in the Table 1.

Table 1
Rate parameters of the PV panel BP SX 100

| | |
|----------------------------------|--------|
| V_{oc} (open circuit voltage) | 32 V |
| I_{sc} (short circuit current) | 5 A |
| V_{pp} (max point voltage) | 24 V |
| P_{pp} (max point power) | 105 W |
| I_{pp} (max point current) | 4.38 A |

Figure 2 shows the current and power versus voltage characteristics of a PV module for $G = 1000, 800, 600, 400$ W/m². For each radiation G the curve has a maximum power point (MPP). To operate the PV system in MPP several techniques have been developed. From Fig. 2 it is noticed that the maximum power has an almost linear relation to the unit of voltage of the network.

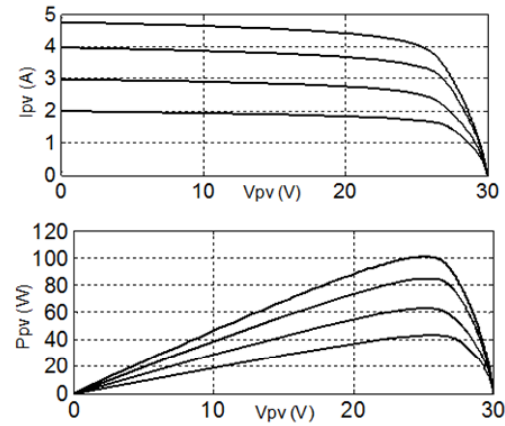


Fig. 2. Current and power versus voltage characteristics

The PV-boost-load system (Fig. 3) using in this section consists of an inductance L , a controlled switch (IGBT), a diode VD and filtering capacitors C . When the switch is on, the boost inductance current increases linearly, the diode VD being blocked. When switch is off, the energy stored in the inductor passes through the diode to the output circuit [19].

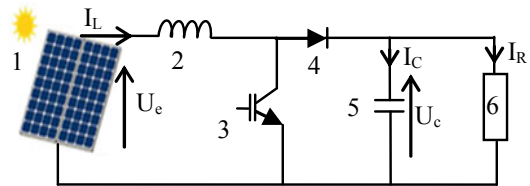


Fig. 3. PV system: 1 – PV panel; 2 – input coil; 3 – IGBT; 4 – diode; 5 – output capacitor; 6 – resistance load

To design the best control law if an appropriate model is chosen. We assume that the continuous conduction mode, the state space average model is given in the following equation [22]:

$$\begin{bmatrix} \dot{x}_1 \\ \dot{x}_2 \end{bmatrix} = \begin{bmatrix} \frac{U_e}{L} - \frac{x_2}{L} \\ \frac{x_1}{C} - \frac{x_2}{RC} \end{bmatrix} + \begin{bmatrix} \frac{x_2}{L} \\ -\frac{x_1}{C} \end{bmatrix} u, \quad (4)$$

where $x_1 = I_L$, $x_2 = U_c$, U_e is the PV voltage, u acts as a control input variable ($0 < u \leq 1$).

The ratio U_c and U_e is given as:

$$\frac{U_c}{U_e} = \frac{1}{u} = \frac{1}{1-D}, \quad (5)$$

where D denotes the duty ratio, and U_c voltage is higher than the U_e voltage.

The Pulse Width Modulation (PWM) signals for driving the switching devices can be generated by comparing the sinusoidal control signal with a triangular carrier signal. The control objective is to design a control law for the control input $u(t)$ such that the output voltage of boost (U_c) attains a desired reference. For the desired set point $x^*=(x_1^* x_2^d)^T$ we get at equilibrium:

$$\begin{cases} x_1^* = \frac{x_2^{d2}}{RU_e} \\ u = 1 - \frac{U_e}{x_2^d} \end{cases} \quad (6)$$

The equation (6) can be written in terms of Port Controlled Hamiltonian (PCH) approach.

Background Port Controlled Hamiltonian. The first work on the PCH has been developed by Dalsmo and van der Schaft in 1992 [20]. It is used to modeling physical systems with lumped-parameter and independent storage elements. Generally, a nonlinear input affine system is described by the following model:

$$\begin{cases} \dot{x} = f(x) + g(x)u \\ y = h(x) \end{cases}, \quad (7)$$

where $f(x)$, $g(x)$ are the Lipschitz functions and x is the states variable such as $\{x \in R^n\}$, $\{h(x) \in C\}$ and $\{(u, y) \in R^{m \times m}\}$.

A system (7) is passive if the inflow of electrical power is always nonnegative and has a property of stability with a positive storage function defined as:

$$H \in C : R^n \rightarrow R_+ / H(x) = \frac{1}{2} x^T Q x, \forall x.$$

where $Q \geq 0$ is the diagonal matrix and such that for $t_1 \geq t_0$ satisfies the inequality:

$$H(x(t_1)) - H(x(t_2)) \leq \int_{t_0}^{t_1} u^T y \Rightarrow \dot{H} \leq u^T y; \forall (x, u, y).$$

For any nonlinear system described by (7) with a storage function $H(x)$ can be modeled as port controlled Hamiltonian system, which is in the simplest and explicit version of the form (8) [11]:

$$\begin{cases} \dot{x} = [J(x) - R(x)] \nabla H(x) + g(x)u \\ y = g^T(x) \nabla H(x) \end{cases}, \quad (8)$$

where $J(x) = -J^T(x) \in R^{m \times n}$ is the interconnection structure matrix, $R(x) = R^T(x) \in R^{m \times n} \geq 0$ is the dissipation matrix and $H(x) : R^n \rightarrow R^+$ is the energy (Hamiltonian) function such as the gradient vector is:

$$\nabla H(x) = \left[\frac{\partial H(x)}{\partial x} \right].$$

From management structure of (8), the acquisition port is $(u^T y)$ [8]. Using evaluating the rate of change energy and version of Kalman-Yakubovich-Popov lemma [21-26], we easily see that PCH model is passive because:

$$\dot{H}(x) = \nabla H^T(x) \dot{x} = u^T y - R(x) (\nabla H(x))^2 \leq u^T y.$$

Moreover:

$$\begin{cases} \nabla H^T(x) f(x) = -R(x) (\nabla H(x))^2 \leq 0 \\ y(x) = g^T(x) \nabla H(x) \end{cases}, \quad (9)$$

In previous sections, a suitable model (4) for boost converter with PCH description is expressed [11, 23-25].

We can write (4) in PCH model as

$$\dot{x} = [J(u) - R] \nabla H(x) + G,$$

where:

$$J(u) = \begin{bmatrix} 0 & \frac{u-1}{LC} \\ -\frac{u-1}{LC} & 0 \end{bmatrix} \in R^{2 \times 2}; \quad R = \begin{bmatrix} 0 & 0 \\ 0 & \frac{1}{RC^2} \end{bmatrix} > 0 \in R^{2 \times 2};$$

$$G = \begin{bmatrix} \frac{U_e}{L} \\ 0 \end{bmatrix} \in R^{2 \times 1}$$

is the constant vector containing the external voltage source.

We assume that the condition ($\omega L \ll 1/(\omega C)$) is satisfied, the boost converter described in (4) is passive since:

$$U_e x_1 - \frac{x_2^2}{R} - y \leq 0.$$

The storage energy:

$$H(x) = \frac{1}{2} x^T Q x; \quad Q = \begin{bmatrix} L & 0 \\ 0 & C \end{bmatrix};$$

$$\nabla H^T(x) = \begin{bmatrix} \frac{\partial H(x)}{\partial x_1} & \frac{\partial H(x)}{\partial x_2} \end{bmatrix} = [Lx_1 \quad Cx_2];$$

and

$$H(x(t_{i+1})) - H(x(t_i)) \leq \int_{t_i}^{t_{i+1}} x_1 U_e dt$$

where $x_1 \cdot U_e$ is the input power.

The total energy change rate for all $t \geq 0$ is given as:

$$H(x(t)) = H(x(0)) + \int_0^t u^T(\tau) \cdot y(\tau) d\tau - R \cdot \int_0^t \nabla H^2[x(\tau)] d\tau. \quad (10)$$

The storage function $H(x)$ is bounded since (10) shows that we can extract a finite amount of the boost converter energy. The system will eventually stop in a minimum energy point. In fact, the boost converter is a passive system and it can be controlled using the IDA-PBC approach.

The rate of convergence of (10) can be increased by a negative feedback interconnection $u = -k \cdot x$ with $k > 0$ a damping injection gain or modified R via IDA-PBC controller.

Our main idea is to assign the desired closed-loop energy function in the equilibrium point $x^*=(x_1^* x_2^d)^T$ using IDA-PBC.

To get the desired output voltage, the following stages must be obtained:

- find a control action $u = \beta(x) + v$ in close-loop and reshaping the amount dissipated energy through by injecting additional damping resistance $r > 0$ to dump the transient oscillation. So:

$$R_d = \begin{bmatrix} r & 0 \\ 0 & \frac{1}{RC^2} \end{bmatrix}.$$

- shaping the new potential energy provided by the capacitor is needed.

The new desired energy function, which has a strict (local) minimum at x^* , form is:

$$H_d(x(t)) = H(x(0)) + \int_0^t \beta^T(\tau)y(\tau)d\tau + \int_0^t v^T(\tau)y(\tau)d\tau - R_d \int_0^t \nabla H^2[x(\tau)].d\tau$$

where:

$$H_d(x) = \frac{1}{2}L(x_1 - x_1^*)^2 + \frac{1}{2}\gamma C(x_2 - x_2^d)^2; \left. \frac{\partial H_d}{\partial x} \right|_{x=x_d} = 0; \left. \frac{\partial^2 H_d}{\partial x^2} \right|_{x=x_d} > 0.$$

$\gamma > 0$ is the adjustable gain in output potential energy to increasing the rate of convergence of power system.

A block diagram representing IDA-PBC approach is shown in Fig. 4.

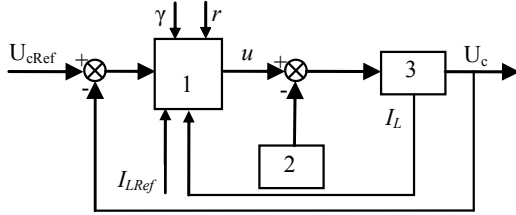


Fig. 4. Scheme of IDA-PBC controller:

1 – IDA-PBC controller; 2 – PWM; 3 – boost with PV cell

The desired target dynamic of (8) is defined as:

$$\dot{x} = (J(u) - R_d) \cdot \nabla H_d(x). \quad (11)$$

Initial conditions and input data. To find a control action (u) in state-feedback for the boost converter, and taking into account all initial conditions ($x(0)$, $u(0)$, $y(0)$) with (11) we make:

$$(J(u) - R_d) \cdot \nabla H_d(x) = (J(u) - R) \nabla H(x) + G. \quad (12)$$

In order to reach a desired voltage x_2^* and for the partial derivative (12) the control law can be found as following:

$$\begin{cases} (u-1)x_2 - \frac{u-1}{\gamma}(x_2 - x_2^d) = -rL^2(x_1 - x_1^*) - U_e; \\ -(u-1)x_1 + (u-1)(x_1 - x_1^*) = \frac{1}{R}x_2 - \frac{1}{R\gamma}(x_2 - x_2^d). \end{cases}$$

So:

$$u = 1 - \gamma \frac{R(x_2^d - U_e)(rL^2x_1 + U_e) - rL^2x_2^{d2}}{R(x_2^d - U_e)(x_2^d + (\gamma-1)x_2)}. \quad (13)$$

In order to choose the optimal values for r and γ we make the initial condition that $0 < u \leq 1$.

So:

$$\begin{cases} r \geq \frac{R(x_2^d - U_e)U_e}{L^2(x_2^{d2} - Rx_1(x_2^d - U_e))} \geq 0 \\ \gamma = \frac{U_e Rx_2^d(x_2^d - U_e)(x_2^d - x_2)}{Rx_2^d(x_2^d - U_e)(rL^2x_1 + U_e) - rL^2x_2^{d3} - U_e Rx_2^d x_2} \end{cases}$$

To eliminate steady state error an integral action is added:

$$u = 1 - \gamma \frac{R(x_2^d - U_e)(rL^2x_1 + U_e) - rL^2x_2^{d2}}{R(x_2^d - U_e)(x_2^d + (\gamma-1)x_2)} + K_p(x_2 - x_2^d) + K_I \int (x_2 - x_2^d)$$

where $(K_p, K_I) \in R^{+*2}$.

Stability analysis. To study the stability of the proposed control we use the Lyapunov theory. If we

assume that $H_d(x)$ is a candidate function of Lyapunov, the asymptotic stability of set (x_1^*, x_2^d) can be investigated such that:

$$H_d(x) = \frac{1}{2}L(x_1 - x_1^*)^2 + \frac{1}{2}\gamma C(x_2 - x_2^d)^2 \geq 0.$$

$$\text{Quadratic function: } \frac{dH_d(x(t))}{dt} = \nabla H_d^T(x) \dot{x}(t).$$

Using (11):

$$\frac{dH_d(x(t))}{dt} = \nabla H_d^T(x) J(u) \nabla H_d(x) - \nabla H_d^T(x) R_d \nabla H_d(x).$$

For $J(u) = -J^T(u)$ we get:

$$\frac{dH_d(x(t))}{dt} = -\nabla H_d^T(x) R_d \nabla H_d(x) \Rightarrow$$

$$\Rightarrow \frac{dH_d(x(t))}{dt} = - \left[\left(\frac{\partial H(x)}{\partial x_1} \right)^2 r + \left(\frac{\partial H(x)}{\partial x_2} \right)^2 \frac{1}{RC^2} \right] \leq 0$$

Simulations results. The validation of the theoretical analysis has been carried out by the average boost converter model supplied by PV array using Matlab/Simulink (Fig. 5).

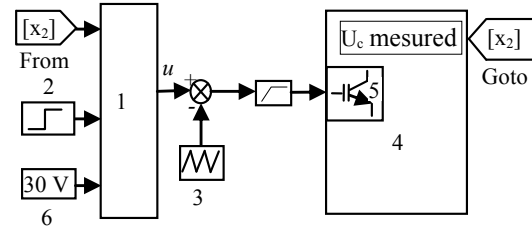


Fig. 5. Simulation diagram of the IDA-PBC:

1 – IDA-PBC controller; 2 – U_{cRef} ; 3 – PWM; 4 – boost converter; 5 – IGBT; 6 – input voltage

The parameters of our system are reported in the Table 2. The virtual resistance should be sufficiently large, to ensure a large energy dissipation amount as well as to minimize the ripples of the current.

Table 2

Parameters of DC-DC boost converter

| Parameter | Values |
|-----------------------|--------------------|
| Input voltage | $U_e = 30$ V |
| Inductance | $L = 54$ mH |
| Capacitor | $C = 4400$ μ F |
| Load resistance | $R = 320$ Ω |
| Integral gain (I) | $K_I = 1.5$ |
| Proportional gain (P) | $K_P = 4$ |
| Dumping resistance | $r = 4$ Ω |
| Adjustable gain | $\gamma = 0.5$ |

In the following, some simulation results are reported in order to show the performances of the proposed controller. The control law is tested with parameters and voltage references variations.

Graphs of changes in output voltage and its reference are shown in Fig. 6.

Referring to Fig. 6, the close loop response adopting IDA-PBC controller exhibit a good tracking of the output voltage to their multivalued reference delivered by PV cell using MPPT algorithm.

Initially the PV voltage is adjusted at 60 V. At time $t = 21.51$ s the reference voltage varies up to 85 V and stabilize in a steady state without error.

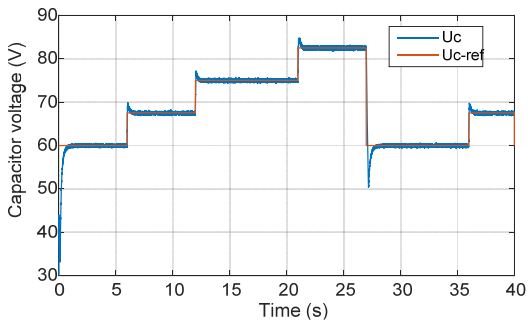


Fig. 6. Simulation results output-voltage during reference voltage variation

Moreover, the reduced duration of the start-up transient operation of the system has been also obtained.

In order to verify the robustness of the proposed method, we will test the performance of IDA-PBC by making variations on parameters system.

According Fig. 7-9 the output voltage does not change with parametric variations; so we deduced the effectiveness robustness of the proposed controller.

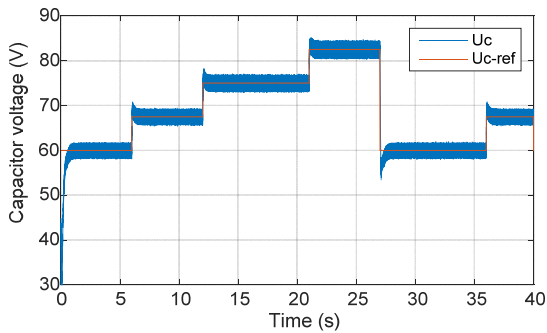


Fig. 7. Output voltage for $\Delta R = 50\%$

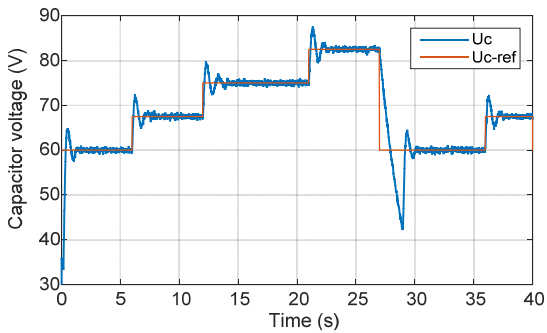


Fig. 8. Output voltage for $\Delta L = 50\%$

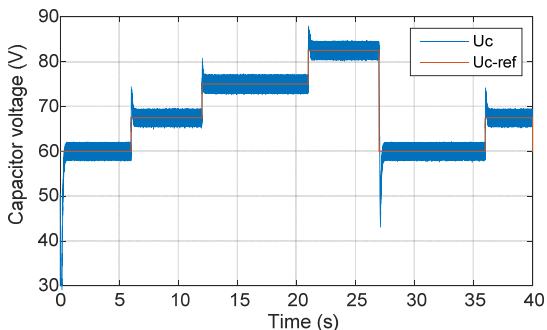


Fig. 9. Output voltage for $\Delta C = 50\%$

Experimental test. To validate the simulations results of proposed control, experiments were conducted on a real system. The layout of the prototype under test is reported in Fig. 10 for obtaining the experimental results.

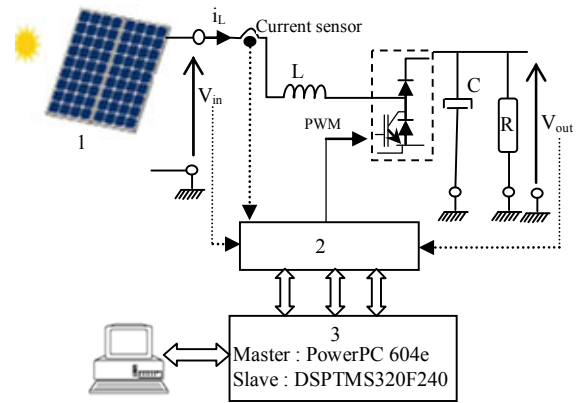


Fig. 10. Laboratory setup structure:
1 – DC source; 2 – interface; 3 – DS1104 dSPACE

The boost converter laboratory structure is based on IGBT modules SKM100GAL123D fed by the DC voltage source. The currents and voltages sensors used are respectively LA-25NP and LV-25P. An interface is used to provide galvanic isolation of all dSPACE DS1103 PPC controller signals (Fig. 11). The main parameters of boost model are reported in Table 3.

Table 3
Experimental parameters of boost converter

| Parameter | Values |
|-----------------------|-------------------------------|
| Input voltage | $U_e = 30\text{ v}$ |
| Inductance | $L = 54\text{ mH}$ |
| Capacitor | $C = 4400\text{ }\mu\text{F}$ |
| Load resistance | $R = 320\text{ }\Omega$ |
| Integral gain (I) | $K_I = 2$ |
| Proportional gain (P) | $K_p = 10$ |
| Dumping resistance | $r = 4\text{ }\Omega$ |
| Adjustable gain | $\gamma = 0.5$ |

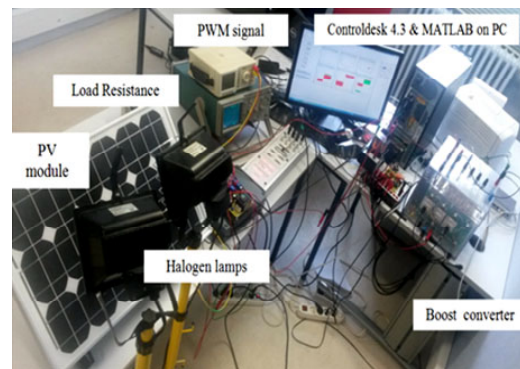


Fig. 11. The hardware setup of the system (LTI laboratory)

Figures 12-15 represents the response output voltage according reference and parameters.

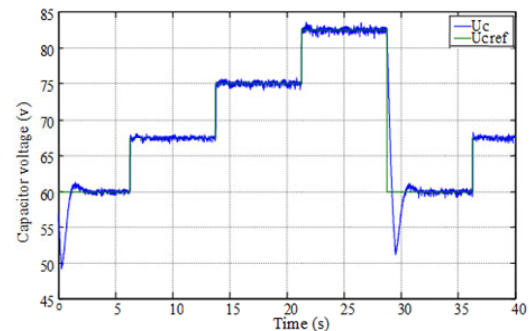


Fig. 12. Output voltage and its reference

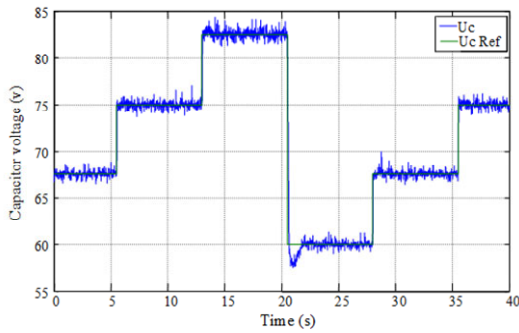


Fig. 13. Output voltage with resistance variation (-50 %)

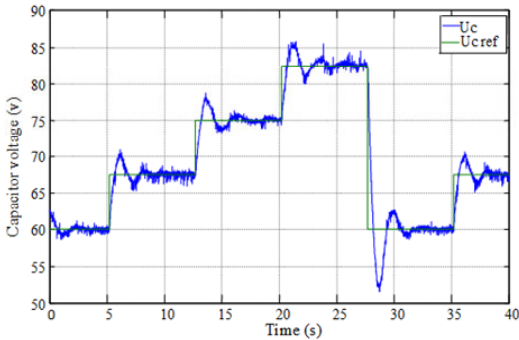


Fig. 14. Output voltage with inductance variation (-50 %)

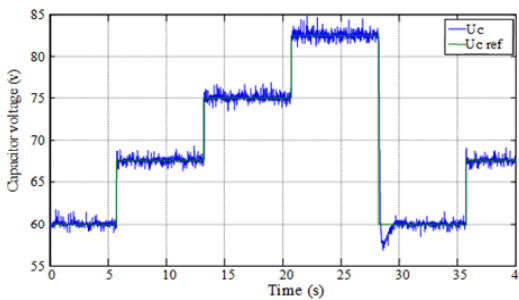


Fig. 15. Output voltage with capacitor variation (-50 %)

The introduced IDA-PBC permits the stability of the system without steady state error (Fig. 16).

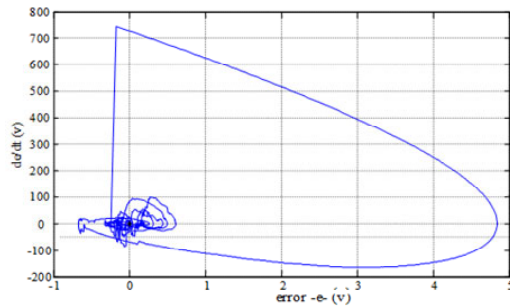


Fig. 16. The trajectory of dynamic error

To validate the proposed control with the classical PI controller a comparative study has been made and the results are presented in Fig. 17, 18.

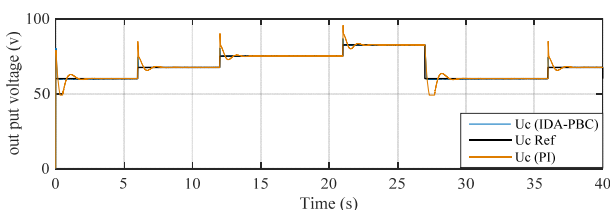


Fig. 17. Output voltage control with PI controller and IDA-PBC

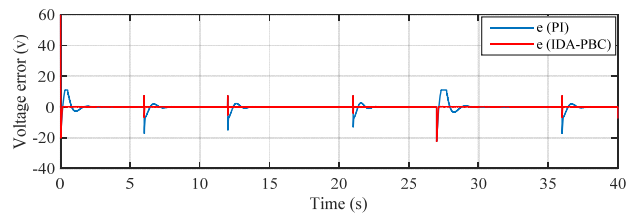


Fig. 18. Dynamic error with PI and IDA-PBC control

Conclusions.

1. The passivity control has been developed to describe energetic properties of dynamical systems and their interconnections; in terms of the input-output behavior and the system is stabilized by an output feedback gain.

2. To design robust controllers via shaping internal energy, we start from the Euler-Lagrange description and then consider instead port-controlled Hamiltonian modeling.

3. To assigning, a desired port controlled Hamiltonian structure in closed-loop the interconnection and damping assignment passivity control technique has turned out to be very successful and has provided solutions of electrical systems.

4. The proposed passivity control has been applied to the DC-DC boost converter and experimental tested on the dSPACE DS1104 system. The general aspects of the performances results are reported and compared with simulation results in order to validate the robustness controller against parameters variation.

5. Our future work revolves around two major challenges: the development of a reliable control of the PV system with fault and the development of controls adapted to the PV system connected to the grid, under constraints.

Conflict of interest. The authors declare that they have no conflicts of interest.

REFERENCES

1. Bennett S. A brief history of automatic control. *IEEE Control Systems Magazine*, 1996, vol. 16, no. 3, pp. 17-25. doi: <https://doi.org/10.1109/37.506394>.
2. S. Bacha, I. Munteanu, A. Iuliana Bratcu. *Power Electronic Converters Modeling and Control with Case Studies*. In *Advanced Textbooks in Control and Signal Processing*. Springer London, 2014. 454 p. doi: <https://doi.org/10.1007/978-1-4471-5478-5>.
3. Petitclair P., Bacha S., Ferrieux J.-P. Optimized linearization via feedback control law for a STATCOM. *IAS '97. Conference Record of the 1997 IEEE Industry Applications Conference Thirty-Second IAS Annual Meeting*, 1997, vol. 2, pp. 880-885. doi: <https://doi.org/10.1109/IAS.1997.628965>.
4. Montoya D.G., Ramos-Paja C.A., Giral R. Improved Design of Sliding-Mode Controllers Based on the Requirements of MPPT Techniques. *IEEE Transactions on Power Electronics*, 2016, vol. 31, no. 1, pp. 235-247. doi: <https://doi.org/10.1109/TPEL.2015.2397831>.
5. Sanders S.R., Verghese G.C. Lyapunov-based control for switched power converters. *21st Annual IEEE Conference on Power Electronics Specialists*, 1990, pp. 51-58. doi: <https://doi.org/10.1109/PESC.1990.131171>.
6. Scherpen J.M.A., Jeltsema D., Klaassens J.B. Lagrangian modeling of switching electrical networks, *Systems & Control Letters*, 2003, vol. 48, no. 5, pp. 365-374. doi: [https://doi.org/10.1016/S0167-6911\(02\)00290-6](https://doi.org/10.1016/S0167-6911(02)00290-6).

7. Kwasinski A., Krein P.T. Passivity-Based Control of Buck Converters with Constant-Power Loads. *2007 IEEE Power Electronics Specialists Conference*, 2007, pp. 259-265, doi: <https://doi.org/10.1109/PESC.2007.4341998>.
8. Ortega R., Lonia A., Nicklasson P.J., Sira-Ramirez H. *Passivity-based Control of Euler-Lagrange Systems: Mechanical, Electrical and Electromechanical Applications*. Springer, 1998. 543 p.
9. Petrovic V., Ortega R., Stankovic A.M. Interconnection and damping assignment approach to control of PM synchronous motors. *IEEE Transactions on Control Systems Technology*, 2001, vol. 9, no. 6, pp. 811-820. doi: <https://doi.org/10.1109/87.960344>.
10. Ortega R., Loria A., Kelly R., Praly L. On passivity-based output feedback global stabilization of Euler-Lagrange systems. *Proceedings of 1994 33rd IEEE Conference on Decision and Control*, 1994, vol. 1, pp. 381-386 doi: <https://doi.org/10.1109/CDC.1994.410898>.
11. Ortega R., Van der Schaft A., Maschke B., Escobar G. Interconnection and damping assignment passivity-based control of port-controlled Hamiltonian systems. *Automatica*, 2002, vol. 38, no. 4, pp. 585-596. doi: [https://doi.org/10.1016/S0005-1098\(01\)00278-3](https://doi.org/10.1016/S0005-1098(01)00278-3).
12. Severn R.P., Bloom G.E. *Modern DC to DC Switch Mode Power Converter Circuits*. Van Nostrand Reinhold, New York, 1982.
13. Venkataramanan R., Sabanovic A., Cuk S. Sliding mode control of DC-to-DC converters. *Proceedings - IECON '85, 1985 International Conference on Industrial Electronics, Control and Instrumentation. Industrial Applications of Mini, Micro & Personal Computers*, 1985, pp. 251-258.
14. Middlebrook R.D., Cuk S. A general unified approach to modelling switching-converter power stages. *1976 IEEE Power Electronics Specialists Conference*, 1976, pp. 18-34, doi: <https://doi.org/10.1109/PESC.1976.7072895>.
15. Montoya D.G., Ramos-Paja C.A., Giral R. Improved Design of Sliding-Mode Controllers Based on the Requirements of MPPT Techniques. *IEEE Transactions on Power Electronics*, 2016, vol. 31, no. 1, pp. 235-247. doi: <https://doi.org/10.1109/TPEL.2015.2397831>.
16. Du W., Jiang Q., Erickson M.J., Lasseter R.H. Voltage-Source Control of PV Inverter in a CERTS Microgrid. *IEEE Transactions on Power Delivery*, 2014, vol. 29, no. 4, pp. 1726-1734. doi: <https://doi.org/10.1109/TPWRD.2014.2302313>.
17. Patcharaprakiti N., Premrudeepreechacharn S. Maximum power point tracking using adaptive fuzzy logic control for grid-connected photovoltaic system. *2002 IEEE Power Engineering Society Winter Meeting. Conference Proceedings*, 2002, vol. 1, pp. 372-377. doi: <https://doi.org/10.1109/pesw.2002.985022>.
18. Ramos-Hernanz J., Uriarte I., Lopez-Guede J.M., Fernandez-Gamiz U., Mesanza A., Zulueta E. Temperature based maximum power point tracking for photovoltaic modules. *Scientific Reports*, 2020, vol. 10, no. 1, p. 3 (12476). doi: <https://doi.org/10.1038/s41598-020-69365-5>.
19. Nebti K., Lebied R. Fuzzy maximum power point tracking compared to sliding mode technique for photovoltaic systems based on DC-DC boost converter. *Electrical Engineering & Electromechanics*, 2021, no. 1, pp. 67-73. doi: <https://doi.org/10.20998/2074-272X.2021.1.10>.
20. Maschke B.M., Van der Schaft A.J. Port-Controlled Hamiltonian Systems: Modeling origins and system theoretic Properties. IFAC Symposia Series, 1993, no. 7, pp. 359-365. doi: <https://doi.org/10.1016/b978-0-08-041901-5.50064-6>.
21. Mendez-Diaz F., Ramirez-Murillo H., Calvente J., Pico B., Giral R. Input voltage sliding mode control of the versatile buck-boost converter for photovoltaic applications. *2015 IEEE International Conference on Industrial Technology (ICIT)*, 2015, pp. 1053-1058. doi: <https://doi.org/10.1109/ICIT.2015.7125236>.
22. Hassan M.A., Li T., Duan C., Chi S., Li E.P. Stabilization of DC-DC buck power converter feeding a mixed load using passivity-based control with nonlinear disturbance observer. *2017 IEEE Conference on Energy Internet and Energy System Integration (EI2)*, 2017, pp. 1-6, doi: <https://doi.org/10.1109/EI2.2017.8245419>.
23. Kassakian J.G., Schlecht M.F., Verghese G.C. *Principles of Power Electronics*. Pearson College Div., 1991. 740 p.
24. Baazouzi K., Bensalah A., Drid S. The PBC technical to control the induction motor. *2014 15th International Conference on Sciences and Techniques of Automatic Control and Computer Engineering (STA)*, 2014, pp. 7-10. doi: <https://doi.org/10.1109/STA.2014.7086690>.
25. Huang J., Wang H. A Passivity-based Control for DC Motor Drive System with PWM. *TELKOMNIKA Indonesian Journal of Electrical Engineering*, 2012, vol. 10, no. 8, pp. 2267-2271. doi: <https://doi.org/10.11591/telkomnika.v10i8.1695>.
26. Escobar G., Van der Schaft A.J., Ortega, R. Hamiltonian viewpoint in the modeling of switching power converters. *Automatica*, 1999, vol. 35, no. 3, pp. 445-452. doi: [https://doi.org/10.1016/S0005-1098\(98\)00196-4](https://doi.org/10.1016/S0005-1098(98)00196-4).

Received 08.12.2021
Accepted 06.03.2022
Published 20.04.2022

Kamel Baazouzi¹, PhD Student of Engineering,
Abed Djebbar Bensalah¹, Doctor of Engineering,
Said Drid², Professor, Dr.-Ing. of Engineering,
Larbi Chrifi-Alaoui³, Dr.-Ing. of Engineering,
¹Electrical Engineering Department
University of Batna 2,
53, Route de Constantine, Fésdis, Batna 05078, Algeria,
e-mail: Baazouzi.kamel@gmail.com (Corresponding Author),
Abedbensalah@yahoo.fr
²Research Laboratory LSPIE,
Electrical Engineering Department,
University of Batna 2,
53, Route de Constantine, Fésdis, Batna 05078, Algeria,
e-mail: saiddrid@iee.org
³Laboratoire des Technologies Innovantes (LTI),
University of Picardie Jules Verne, IUT de l'Aisne,
13 Avenue François Mitterrand 02880 Cuffies-Soissons, France,
e-mail: larbi.alaoui@u-picardie.fr

How to cite this article:

Baazouzi K., Bensalah A.D., Drid S., Chrifi-Alaoui L. Passivity voltage based control of the boost power converter used in photovoltaic system. *Electrical Engineering & Electromechanics*, 2022, no. 2, pp. 11-17. doi: <https://doi.org/10.20998/2074-272X.2022.2.02>